MATHEMATICAL BIOSCIENCES
AND ENGINEERING
Volume **10**, Number **3**, June **2013**

doi:10.3934/mbe.2013.10.821

pp. **821–842**

# MODELING BACTERIAL ATTACHMENT TO SURFACES AS AN EARLY STAGE OF BIOFILM DEVELOPMENT

Fadoua El Moustaid

African Institute for Mathematical Sciences
6 Melrose road, Muizenberg, 7945, South Africa

Amina Eladdadi

The College of Saint Rose, Department of Mathematics
432 Western Avenue, Albany, NY 12203, USA

Lafras Uys

African Institute for Mathematical Sciences
6 Melrose road, Muizenberg, 7945, South Africa

Abstract. Biofilms are present in all natural, medical and industrial surroundings where bacteria live. Biofilm formation is a key factor in the growth and transport of both beneficial and harmful bacteria. While much is known about the later stages of biofilm formation, less is known about its initiation which is an important first step in the biofilm formation. In this paper, we develop a non-linear system of partial differential equations of Keller-Segel type model in one-dimensional space, which couples the dynamics of bacterial movement to that of the sensing molecules. In this case, bacteria perform a biased random walk towards the sensing molecules. We derive the boundary conditions of the adhesion of bacteria to a surface using zero-Dirichlet boundary conditions, while the equation describing sensing molecules at the interface needed particular conditions to be set. The numerical results show the profile of bacteria within the space and the time evolution of the density within the free-space and on the surface. Testing different parameter values indicate that significant amount of sensing molecules present on the surface leads to a faster bacterial movement toward the surface which is the first step of biofilm initiation. Our work gives rise to results that agree with the biological description of the early stages of biofilm formation.

1. **Introduction.** A biofilm is an aggregation of microorganisms that form on both natural and abiotic surfaces, and are irreversibly attached to a substrate or each other and embedded in a matrix of extracellular polymeric substances that they produce [31, 54]. Biofilms are of a great relevance to the medical community since they have been associated with a variety of persistent infections that respond poorly to conventional antibiotic chemotherapy [21]. They are involved in a wide variety of microbial infections, accounting for over 80 percent of microbial infections in the body (according to NIH [59]). Examples of infectious diseases in which biofilms have

2010 *Mathematics Subject Classification.* Primary: 58F15, 58F17; Secondary: 53C35.

*Key words and phrases.* Chemotaxis, bacterial biofilm, Keller-Segel model, sensing molecules.

The first author is supported by The African Institute for Mathematical Sciences (AIMS-South Africa).

been involved include: urinary tract infections, formation of dental plaque, gastrointestinal tract, airway/lung tissue, cystic fibrosis infections, infections of permanent indwelling devices such as joint prostheses and heart valves, and for chronic administration of chemotherapeutic agents, to list just a few [59]. Biofilms are not all bad, they are a natural phenomenon that exists in our everyday environments and can be found even in extremely hot and cold environment. Biofilm can be beneficial, where it can be used, for example, to help in the clean up of an oil spill, in waste water treatment, and in soil remediation [46]. The development of a biofilm is a complicated biological process since it depends strongly on the surrounding environment. The ability of bacteria to attach to surfaces and develop into a biofilm has been of a great interest to both experimentalists and mathematicians. Biofilms have been the subject of mathematical modeling for over 30 years [51]. There are several approaches to modeling biofilms mathematically. Each particular type of biofilm models has its own assumptions and its own computational and mathematical tools. These models usually consider that biofilm's structure is determined by the substrate concentration and bacterial movement and they generally deal with final stages of biofilm formation [42, 51, 48]. This fact makes the models mainly governed by the diffusion process. However, the stage in the biofilm development that has been neglected is the initial bacterial cell attachment to a surface, which is a critical initial step in the biofilm development. The initial attachment is essential for the formation of a bacterial biofilm, as all other cells within a biofilm structure rely on the interaction between surface and bacterial cell for their survival. The focus of this paper is to gain some fundamental understanding of the mechanisms of biofilm initiation. Modeling this particular stage leads to a better understanding of the whole process, which, therefore leads to the ability of either inhibiting a detrimental biofilms or accelerating the formation of a beneficial biofilm. This stage is governed by bacterial chemotaxis towards the sensing molecules that leads to finding the surface and therefore the attachment. To model the biofilm initiation process, we use a Keller-Segel (K-S) type mathematical model for bacterial chemotaxis. Keller and Segel applied their model to a population of *amoeba* chemotactic interaction [15]. Then, they observed a biased bacterial movement in an experiment done on *E. coli* motility [17], before they announced the mathematical model that study bacterial behavior and named after them (for a history on the K-S model see for example [14]). Our K-S type model is composed of two partial differential equations describing the collective motion of bacterial cells that are attracted by a chemical substance and are able to emit it. The first equation involves bacterial density diffusion, chemotaxis toward the attractant as well as the growth and death. The second equation concerns the attractant (or the repellent) diffusion degradation and production. The quantities are left in their general form so that they can fit any biological context [7, 34, 16].

This paper is organized as follows: the background section 2 presents the biology (sec. 2.1) and development of bacterial biofilms (sec. 2.2), and a brief literature review on previous mathematical models of bacteria (2.3). Our mathematical model on biofilm initiation is introduced in section 3. Section 4 describes the derivation of the initial and boundary conditions. Non-dimensionalization is presented in section 5. Numerical results and model predictions are discussed in section 6. In section 7, the bacterial growth is added to the coupled model of chemotaxis, and the model is presented in one dimensional space. The conclusion and future work are shown in section 8

## 2. Background.

2.1. **Biofilm biology.** Biofilms are small communities of bacterial cells that can grow on either, rich-nutrient or poor-nutrient surfaces. They can form floating mats on liquid surfaces and also on interfaces like air-water interfaces [2]. Biofilms can be made up of many different microorganisms such as bacteria, fungi, protozoa, algae, archaea with associated bacteriophages and other viruses [31, 54]. Each group performs specialized metabolic functions. However, some organisms will form single-species films under certain conditions. Biofilms surround themselves by a slime they secrete, generally composed of a matrix of excreted polymeric compounds called extracellular polymeric substance. This matrix protects the cells within it and facilitates communication among them through biochemical signals [49]. Biofilms have a complex social structure, and are known for their structural heterogeneity and genetic diversity [54]. They also show a changed phenotype with respect to the growth rate and gene transcription [31, 54]. Biofilm can form on and adhere to nearly any surface such as plaque on teeth, piping / plumbing, catheters, medical devices, etc. Biofilms provide an easy way for bacteria to find food and nutrients, as well as a high tolerance to antibiotics [47]. Within a biofilm the cells are more cooperative with each other and behave differently than when they are in the free-state [30]. In fact, bacteria of the same species are much more antimicrobial resistant, within a biofilm than in the free-swimming state. This is because of the high cooperation between the biofilm members. Two positive facts making bacteria choose to live within a biofilm instead of the planktonic state, are: (1) the ability to differentiate into types that differ in their nutrient requirements, which means there are fewer competitors for a particular nutrient; (2) when conditions deteriorate in a biofilm, some bacteria sacrifice themselves for the other bacteria to have a better life. They become planktonic cells once again, looking for another surface and build another biofilm in better conditions [33].

2.2. **Biofilm development.** Biofilm development is a multi-stage process which begins when free-swimming (planktonic) bacteria encounter a surface, and occurs in a sequential process of five stages, which are: initial attachment or adsorption to the surface, irreversible attachment, first maturation, second maturation, and dispersion [56, 36]. Figure 1 depicts the five stages of the biofilm formation

The first stage is the initial attachment, where the bacteria move toward either a living or non-living surface and attach to it. In the life and times of the biofilm, the initial adhesion of the planktonic bacterial cell to a conditioned surface is considered as a random event [38]. This free-living bacteria produce sensing molecules as they move through the bulk fluid. These chemicals become significantly concentrated as the population of bacteria grows, they diffuse radially away from the floating cells and get reflected once they reach the surfaces. At this stage, bacteria sense their proximity to these surfaces because diffusion had become limited on that side [8, 25]. The bacteria keep moving toward the nearest surface where they get stuck, resulting in more sensing molecules produced at the boundaries. This increased production causes an escalation in the recruitment of bacteria to the pioneering colonies, which will merge to form the biofilm [51].

The second stage is the irreversible attachment where bacteria produce the polysaccharide matrix to facilitate their movement to a swarming rather than a free-state. The third stage is a period of the first maturation, which consists of

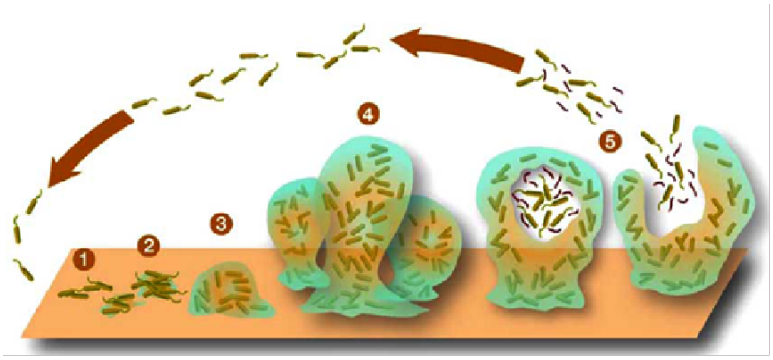


FIGURE 1. Description of the biofilm life cycle that occurs in five stages described in details in the text.
Source: http://prometheus.matse.illinois.edu/glossary/biofilms/.

growing as an initiated biofilm; bacteria proliferate and differentiate and also welcome other bacteria to join them. The fourth stage of development is the second maturation phase, in which the biofilm reaches its maximum thickness. This is also the point at which biofilm bacteria are profoundly different from planktonic bacteria with respect to the number of differentially expressed proteins [36]. The final stage is dispersion, which an essential stage of the biofilm life cycle, at which the cells disperse from the biofilm colony. This stage enables biofilms to spread and colonize new surfaces, and this occurs when the environmental conditions worsen and bacteria choose to detach from the biofilm either to look for other surfaces or to join another biofilm. The developmental life cycle of biofilm comes full circle when dispersed biofilm cells revert to the planktonic mode of growth [30, 46, 36].

Biofilm cells were shown to change regulation of motility, alginate production, and quorum sensing during the process of development [36]. In the natural world, bacteria are more likely to grow and survive in organized communities than to be found as isolated cells [28, 20]. This free-living bacteria produce sensing molecules as they move through the bulk fluid. These molecules become significantly concentrated as the population of bacteria grows, they diffuse radially away from the floating cells and get reflected once they reach the surfaces [30]. At this stage, bacteria sense their proximity to these surfaces because diffusion had become limited on that side [23]. The bacteria keep moving toward the nearest surface where they get stuck, resulting in more sensing molecules produced at the boundaries. This increased production causes an escalation in the recruitment of bacteria to the pioneering colonies, which will merge to form the biofilm [21].

2.3. **Previous mathematical models.** Over the last 30 years, a good progress has been made in the mathematical modeling of bacterial biofilms. There are several approaches to modeling biofilms mathematically. Biofilm can be modeled as a quantity that is continuous, discrete or both depending on the situation described. The models have been classified into roughly four categories, namely, low-dimensional continuum models, diffusion-limited aggregation models (see for example [51]), continuum-discrete models (see for example [13]) and fully-coupled biofilm-fluid models [5]. The one-dimensional continuum models involve quantities

assumed to be continuous, in time and on one-dimensional space. This category of models usually deals with steady-state biofilm growth dynamics, which includes: the biofilm's thickness; the spatial distribution of bacterial species, and substrate concentration The second category simply describe the shape of biofilms these have variously been described as looking like mushrooms, towers, fractals or some other pattern (see for example [48, 55]). Most of these models are computational such as Diffusion Limited Aggregation (DLA) or Cellular Automata models. They are based on the movement and positions of bacteria within a well defined space [40, 42, 6]. The third type deals with biofilm growth, either by considering the biofilm as a continuum mass growing, or by taking into account the interaction between the individuals [35, 23, 48]. These models vary from continuum to discrete type. A fourth type, is those models that couple the biofilm and the surrounding environment, usually a fluid. These studies include biofilm sloughing and shear stress which also play an important role in biofilm life cycle. In general, these models are discrete-continuum or fully coupled biofilm-fluid models (see for example [38, 41, 8, 23, 18]).

3. **Mathematical model.** In this section we present the coupled mathematical model describing bacterial density and sensing molecules concentration. We do not consider bacterial growth in this model. First, we define the main equations while the boundary and initial conditions are presented later on in section 4. Before presenting our model, we first give a brief description of how we link the biology of biofilm formation with the process of the mathematical modeling. The movement of free-bacteria is a biased random walk toward sensing molecules. This is described using the concept of chemotaxis, which leads to a Keller-Segel type model. The production of sensing molecules occurs in the free-space and at the surface, which is represented by functions that depend on bacterial densities and fixed rates of production. For sensing molecules degradation, this is presented by a linear function of molecules concentration. The bacterial stickiness is modeled by zero-Dirichlet boundary conditions. While the function describing sensing chemicals at the surface (boundary conditions) will be explained in details in section 4. In reality, there are other facts that occur during the bacterial attachment to surfaces and biofilm initiation that need to be considered simultaneously by the model, such as: (i) the production of sensing molecules in the free-space and at the surface, (ii) the diffusion and degradation of sensing molecules over time, and space, and (iii) bacterial movement towards sensing molecules, this biological behavior is called chemotaxis [10, 23].

First, we consider a spherical domain, $\Omega$, of center 0 and radius $R$. The variables and parameters used throughout this paper are presented in Table 1. The mathematical model does not consider bacterial growth and is presented in Cartesian coordinates by:

$$\begin{aligned} \frac{\partial b}{\partial t}(\mathbf{x},t) &= D_b\nabla^2 b - \chi\nabla(b\nabla s), && \text{in } \Omega\times(0,+\infty),\\ \frac{\partial s}{\partial t}(\mathbf{x},t) &= D_s\nabla^2 s - \lambda s + \alpha b, && \text{in } \Omega\times(0,+\infty), \end{aligned}$$

where all the parameters are constants and presented in Table 1 and $\mathbf{x} = (x, y, z) \in \Omega$. The first equation describes bacterial random walk using the diffusion equation. Bacterial chemotaxis is presented by the term $-\dfrac{\partial J_c}{\partial \mathbf{x}}$, where $J_c$ is the chemotactic

TABLE 1. State parameters and variables used in this paper.

| Parameter | Description | Unit |
|---|---|---|
| $a$ | Bacterial growth rate | $1/s$ |
| $b, B, B_0$ | Bacterial density | $kg/m^3$ |
| $D_b$ | Bacterial diffusivity | $m^2/s$ |
| $D_s$ | Sensing molecules diffusivity | $m^2/s$ |
| $F$ | Logistic function of bacterial density | $kg/m^3$ |
| $g$ | Proportion of stuck-bacteria per time $t$ | $mol/m^2\ s$ |
| $K$ | Bacterial carrying capacity | $kg/m^3$ |
| $L$ | Non-dimensionalized parameters | No unit |
| $M$ | Non-dimensionalized parameters | No unit |
| $s, S, S_0$ | Sensing molecules concentration | $mol/m^3$ |
| $\alpha$ | Sensing molecules production rate in the free-space | $mol/kg\ s$ |
| $\beta$ | Sensing molecules production rate in the boundaries | $m\ mol/kg\ s$ |
| $\lambda$ | Sensing molecules degradation rate | $1/s$ |
| $\mu$ | Fixed rate of bacterial stickiness | $1/m\ kg$ |
| $\chi$ | Chemotactic coefficient | $m^5/mol\ s$ |
| $\pi$ | Intermediate function | $kg/m^3$ |

flux given by $J_c = \chi b \dfrac{\partial s}{\partial x}$ with $\chi$ the chemotactic coefficient. In the second equation we describe sensing molecules diffusion, degradation and production.

For simplicity, we write the model in spherical coordinates so that the uniform initial distribution of bacterial density and sensing molecules concentration to ensure a radial symmetry for our variables, which means that the dependence will only be with respect to the sphere radius. Let us consider the following change of variables:

$$b(x, y, z, t) = b(r\sin\theta\cos\varphi, r\sin\theta\sin\varphi, r\cos\theta, t) = B(r, \theta, \varphi, t), \tag{1}$$

$$s(x, y, z, t) = b(r\sin\theta\cos\varphi, r\sin\theta\sin\varphi, r\cos\theta, t) = S(r, \theta, \varphi, t), \tag{2}$$

where $r \in [0, R]$, $\theta \in [0, \pi]$ and $\varphi \in [0, 2\pi]$. Because of the radial symmetry we have:

$$B(r, \theta, \varphi, t) = B(r, t), \tag{3}$$

$$S(r, \theta, \varphi, t) = S(r, t). \tag{4}$$

The model is then reduced to the following:

$$\frac{\partial B}{\partial t} = \frac{D_b}{r^2}\frac{\partial}{\partial r}(r^2\frac{\partial B}{\partial r}) - \chi(\frac{\partial B}{\partial r}\frac{\partial S}{\partial r} + \frac{B}{r^2}\frac{\partial}{\partial r}(r^2\frac{\partial S}{\partial r})), \qquad 0 < r < R,\ t > 0, \tag{5}$$

$$\frac{\partial S}{\partial t} = \frac{D_s}{r^2}\frac{\partial}{\partial r}(r^2\frac{\partial S}{\partial r}) - \lambda S + \alpha B, \qquad 0 < r < R,\ t > 0. \tag{6}$$

Now that our main equations are defined we should give the model the appropriate boundary and initial conditions. This will be the subject of the next section (sec 4).

4. **Initial and boundary conditions.** In this section, we consider the bacterial density and sensing molecules dynamics at the surface. Bacteria are assumed to be stuck once the surface is reached, which means that we use adsorbing boundary conditions. The sensing molecules have more than one behavior happening at the same time, that is, they diffuse, get produced, and degrade at the surface [30]. To express this mathematically we need to build our own boundary conditions, which

are detailed below at $r = 0$ and $r = R$.

**At $r = 0$:** Starting from a uniform distribution for both bacteria and sensing molecules, the variables are radially symmetric which insure that the flux coming in at $r = 0$ is the same as the one going out. For that, we consider the zero-Neumann boundary conditions at $r = 0$, given by:

$$\frac{\partial B}{\partial r}(0,t) = 0, \qquad t > 0, \tag{7}$$

$$\frac{\partial S}{\partial r}(0,t) = 0, \qquad t > 0. \tag{8}$$

**At $r = R$:** For bacteria, we use zero-Dirichlet boundary conditions at $r = R$. Assuming that the surface where bacteria get stuck is actually the sphere surface, i.e:

$$B(R,t) = 0, \quad t > 0. \tag{9}$$

For sensing molecules, the boundary condition at $r = R$ is much more complicated, since there are many biochemical processes happening simultaneously. At the surface, sensing molecules degrade, diffuse and are produced by both free-bacteria and stuck-bacteria. To distinguish between the two we consider sensing production by free-bacteria as their growth and stuck-bacteria as a source.

To derive the equation at the boundaries we need to use the conservation equation, which is defined in a given volume. In our case, we take a spherical cap $V$ to be our domain. $V$ is defined as follows:

$$V = \{(r,\theta,\varphi),\ R - \Delta r \le r \le R; \Theta - \Delta\theta \le \theta \le \Theta + \Delta\theta; \Phi - \Delta\varphi \le \varphi \le \Phi + \Delta\varphi\},$$

So that after $\Delta r$, $\Delta\theta$ and $\Delta\varphi$ approach zero, we obtain the equation of sensing molecules at the point $(R,\theta,\varphi)$ which is the same for all the points on the sphere surface. The conservation equation gives:

$$\underbrace{\frac{\partial}{\partial t}\int_V S dV}_{LHS} = \underbrace{\underbrace{-\int_{\partial V} J\partial V}_{Sensing\ chemicals\ flux} + \underbrace{\int_V f(S,B)dV}_{Growth\ and\ degradation} + \underbrace{\int_{\partial V} g(t)\partial V}_{Source\ at\ surface}}_{RHS}, \tag{10}$$

where,

$$\begin{cases} \partial V = S_{base} + S_{lateral} + S_{top}, \\ f(S,B) = -\lambda S + \alpha B, \\ g(t) = \beta B_{wall}(t) = \beta(B_0 - \int_0^R B(r,t)dr). \end{cases}$$

The $S_{base}$ and $S_{top}$ are the base and top surfaces of the spherical cap respectively, and the $S_{lateral}$ are the four surfaces around the spherical cap defined by $\theta$ and $\varphi$. Because of the radial symmetry, the fluxes coming into the volume $V$ through the lateral surfaces are equal to the fluxes going out, so that they cancel each other. On left side, the quantity in the LHS leads to:

$$\begin{aligned} \frac{\partial}{\partial t}\int_V S dV &= \int_V \frac{\partial S}{\partial t} dV, \\ &= \int_V D_s \frac{\partial^2 S}{\partial r^2} dV + \int_V f(S,B)dV, \end{aligned}$$

using the Divergence theorem we obtain:

$$\begin{aligned}\int_V D_s\frac{\partial^2 S}{\partial r^2}dV + \int_V f(S,B)dV &= \int_{\partial V} D_s\frac{\partial S}{\partial r}\partial V + \int_V f(S,B)dV,\\ &= \int_{S_{base}} D_s\frac{\partial S}{\partial r}dS + \int_{S_{lateral}} D_s\frac{\partial S}{\partial r}dS\\ &+ \int_{S_{top}} D_s\frac{\partial S}{\partial r}dS + \int_V f(S,B)dV,\end{aligned}$$

since the lateral fluxes cancel each other, the final expression is then given by:

$$\frac{\partial}{\partial t}\int_V SdV = \int_{S_{base}} D_s\frac{\partial S}{\partial r}dS + \int_{S_{top}} D_s\frac{\partial S}{\partial r}dS + \int_V f(S,B)dV. \tag{11}$$

On the right side, the quantity in the RHS gives rise to:

$$\begin{aligned}\underbrace{-\int_{\partial V} J\partial V}_{Sensing\ chemicals\ flux} &= -\{\int_{S_{base}} JdS + \int_{S_{lateral}} JdS + \int_{S_{top}} JdS\},\\ \underbrace{\int_V f(S,B)dV}_{Growth\ and\ degradation} &= \int_V f(S,B)dV,\\ \underbrace{\int_{\partial V} g(t)\partial V}_{Source\ at\ surface} &= \int_{S_{base}} g(t)dS + \int_{S_{lateral}} g(t)dS + \int_{S_{top}} g(t)dS,\end{aligned}$$

The source term $g(t)$ represents the bacterial density at the surface at each time $t$. It consists of bacterial growth on the surface as well as bacteria coming from the free-space and stuck on the surface. The source from the stuck-bacteria makes lateral and base sources equal to zero, again the lateral fluxes cancel each other and there is no flux coming from the top surface, so that we can write:

$$\begin{aligned}\underbrace{-\int_{\partial V} J\partial V}_{Sensing\ chemicals\ flux} &= -\int_{S_{base}} JdS = \int_{S_{base}} D_s\frac{\partial S}{\partial r}dS,\\ \underbrace{\int_V f(S,B)dV}_{Growth\ and\ degradation} &= \int_V f(S,B)dV,\\ \underbrace{\int_{\partial V} g(t)\partial V}_{Source\ at\ surface} &= \int_{S_{top}} g(t)dS,\end{aligned}$$

which is equivalent to:

$$\begin{aligned}\underbrace{-\int_{\partial V} J\partial V}_{Sensing\ chemicals\ flux} + \underbrace{\int_V f(S,B)dV}_{Growth\ and\ degradation} + \underbrace{\int_{\partial V} g(t)\partial V}_{Source\ at\ surface}\\ = \int_{S_{base}} D_s\frac{\partial S}{\partial r}dS + \int_V f(S,B)dV + \int_{S_{top}} g(t)dS,\end{aligned}$$

Taken together with equation (11), equation (10) becomes:

$$\int_{S_{base}} D_s \frac{\partial S}{\partial r} dS + \int_{S_{top}} D_s \frac{\partial S}{\partial r} dS + \int_V f(S,B) dV = \int_{S_{base}} D_s \frac{\partial S}{\partial r} dS + \int_V f(S,B) dV + \int_{S_{top}} g(t) dS,$$

Thus:

$$\int_{S_{top}} D_s \frac{\partial S}{\partial r} dS = \int_{S_{top}} g(t) dS, \tag{12}$$

which we integrate in spherical coordinates to finally obtain:

$$D_s \frac{\partial S}{\partial r}(R,t) - \beta(B_0 - \int_0^R B(r,t) dr) = 0, \quad t > 0. \tag{13}$$

This type of boundary conditions is called Robin boundary conditions. Our boundary conditions at $r = R$ are summarized as follows:

$$B(R,t) = 0, \quad t > 0, \tag{14}$$

$$D_s \frac{\partial S}{\partial r}(R,t) - \beta(B_0 - \int_0^R B(r,t) dr) = 0, \quad t > 0. \tag{15}$$

To explain the biological interpretation of equation (15) we consider the followings:

$$D_s \frac{\partial S}{\partial r}(R,t) - \beta(B_0 - \int_0^R B(r,t) dr) = 0, \tag{16}$$

$$\Rightarrow \quad \frac{\partial S}{\partial r}(R,t) = \frac{\beta}{D_s}(B_0 - \int_0^R B(r,t) dr), \tag{17}$$

$$\Rightarrow \quad \frac{S(R,t) - S(R-\Delta r,t)}{\Delta r} \approx \frac{\beta}{D_s}(B_0 - \int_0^R B(r,t) dr), \tag{18}$$

$$\Rightarrow \quad S(R,t) - S(R-\Delta r,t) \approx \frac{\beta}{D_s} \Delta r (B_0 - \int_0^R B(r,t) dr). \tag{19}$$

Depending on the sensing molecules diffusivity $D_s$ and the sensing molecules production rate $\beta$ we have four cases:

**When $\beta$ increases:** this implies that $S(R,t) \gg S(R-\Delta r,t)$, which means that there is a high production of sensing molecules at the surface so that the sensing molecules concentration at the surface is much higher than in the free-space.

**When $\beta$ decreases:** this is equivalent to $S(R,t) \approx S(R-\Delta r,t)$. In this case, the production of sensing molecules at the surface is very low so that the concentration is approximately the same in the free-space and at the surface.

**When $D_s$ increases:** this indicates that $S(R,t) \approx S(R-\Delta r,t)$. In other words, when the sensing molecules diffusivity is high, the sensing molecules move very fast and are able to displace from the surface where they are produced to the free-space.

**When $D_s$ decreases:** this means that $S(R,t) \gg S(R-\Delta r,t)$, that is when sensing molecules diffusivity is small the movement of sensing molecules is very slow which explains that they spend more time at the surface before moving to the free-space. See Figure 2.

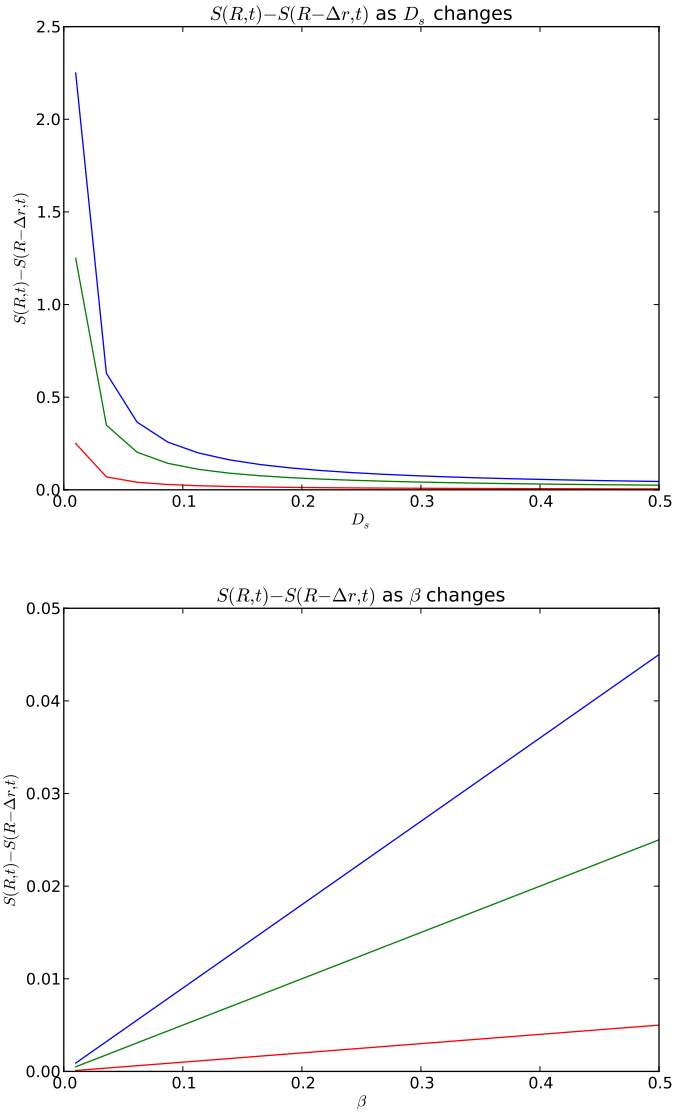


FIGURE 2. The figure shows the change in $S(R,t)-S(R-\Delta r,t)$ as the parameters $D_s$ and $\beta$ change their values. The parameter values used are $R = 1$, $\Delta r = 0.05$, $B_0 = 0.9$ and three different times $t = 0, t = 500$, and $t = 1000$. All the three curves agree with the analytical discussion. As the diffusivity parameter $D_s$ gets larger, the sensing molecules move faster toward the free-space, and when $D_s$ gets smaller the sensing molecules are rather stationary. For the production rate $\beta$, the dependence is linear, the more production of sensing molecules we have the higher is their concentration at the surface than it is in the free-space and vice versa.

For initial conditions, we assume that the bacteria start in a uniform distribution with a very low amount of sensing molecules present, so that:

$$\begin{aligned} B(r,0) &= B_0, && 0 < r < R, \\ S(r,0) &= S_0, && 0 < r < R, \end{aligned}$$

where $B_0$ is the bacterial density, and $S_0$ is sensing molecules concentration at $t = 0$ (constants defined in Table 1).

5. **Non-dimensionalization.** Since the mathematical model involves measured parameters and variables, we first non-dimensionalize it before studying it further. To non-dimensionalize equations (5) and (6), we introduce the non-dimensional variables $B^*$, $S^*$, $x^*$, and $t^*$ defined by:

$$t = \omega t^*, \quad B = B_0 B^*, \quad S = S_0 S^*, \quad r = R r^*. \tag{20}$$

Rewriting equations (5) and (6) in terms of these new non-dimensional variables, we get:

$$\frac{R^2}{D_b \omega}\frac{\partial B^*}{\partial t^*} = \frac{1}{r^{*2}}\frac{\partial}{\partial r^*}(r^{*2}\frac{\partial B^*}{\partial r^*}) - \frac{\chi S_0}{D_b}(\frac{\partial B^*}{\partial r^*}\frac{\partial S^*}{\partial r^*} + \frac{B^*}{r^{*2}}\frac{\partial}{\partial r^*}(r^{*2}\frac{\partial S^*}{\partial r^*})) \tag{21}$$

$$\frac{1}{\lambda\omega}\frac{\partial S^*}{\partial t^*} = \frac{D_s}{R^2\lambda}\frac{1}{r^{*2}}\frac{\partial}{\partial r^*}(r^{*2}\frac{\partial S^*}{\partial r^*}) - S^* + \frac{\alpha B_0}{\lambda S_0}B^* \tag{22}$$

with boundary conditions given by:

$$\frac{\partial B^*}{\partial r^*}(0,t^*) = \frac{\partial S^*}{\partial r^*}(0,t^*) = 0, \tag{23}$$

$$B^*(1,t^*) = 0, \quad \frac{\partial S^*}{\partial r^*}(1,t^*) = \frac{\beta\chi}{D_s D_b}B_0 - \frac{\beta\lambda}{D_s\alpha}\int_0^1 B^*(r^*,t^*)dr^*, \tag{24}$$

and initial conditions:

$$B^*(r^*,0) = \frac{B_0\alpha\chi}{D_b\lambda} = B_0^*, \tag{25}$$

$$S^*(r^*,0) = \frac{S_0\chi}{D_b} = S_0^*. \tag{26}$$

This form suggests the choices of the following constants:

$$\omega = \frac{D_s}{D_b\lambda}, \quad R = \sqrt{\frac{D_s}{\lambda}}, \quad S_0 = \frac{D_b}{\chi}, \quad B_0 = \frac{D_b\lambda}{\alpha\chi}. \tag{27}$$

Furthermore, we define the three non-dimensional parameters $\tau$, $L$ and $M$, as follows:

$$\tau \equiv \frac{D_b}{D_s}, \quad L \equiv \frac{R\beta\chi B_0}{D_s D_b}, \quad M \equiv \frac{\beta\lambda}{D_s\alpha}. \tag{28}$$

Using these new variables, and dropping the asterisks for simplicity, we obtain the non-dimensionalized system of equations that describes the biofilm initiation stage:

$$\begin{cases} \dfrac{\partial B}{\partial t} = \dfrac{1}{r^2}\dfrac{\partial}{\partial r}(r^2\dfrac{\partial B}{\partial r}) - (\dfrac{\partial B}{\partial r}\dfrac{\partial S}{\partial r} + \dfrac{B}{r^2}\dfrac{\partial}{\partial r}(r^2\dfrac{\partial S}{\partial r})), \\ \tau\dfrac{\partial S}{\partial t} = \dfrac{1}{r^2}\dfrac{\partial}{\partial r}(r^2\dfrac{\partial S}{\partial r}) - S + B, \\ \dfrac{\partial B}{\partial r}(0,t) = \dfrac{\partial S}{\partial r}(0,t) = 0, \\ B(1,t) = 0, \quad \dfrac{\partial S}{\partial r}(1,t) - (L - M\displaystyle\int_0^1 B(r,t)dr) = 0, \\ B(r,0) = B_0, \\ S(r,0) = S_0. \end{cases} \tag{29}$$

Model variables and constants are summarized in Table 1. Next, we solve the mathematical model numerically and present some simulation results (in sec. 6).

6. **Numerical results.** The model presented in this paper involves both bacteria and the presence of sensing molecules which direct bacterial movement, this phenomenon is known as chemotaxis. The presence of chemotaxis in the model makes the Keller-Segel type model difficult to study analytically. Instead, we choose to study our model numerically. For that we first non-dimensionalized the equations to remove the units and reduce the number of parameters, then simulated the model using Matlab. Even numerically, it is not easy to study system (29). The term $1/r^2$ represents a singularity problem when $r$ is very small. To avoid this type of singularity, we use the function *Pdepe* in Matlab which solves initial-boundary value problem for system of parabolic-elliptic partial differential equations. So implementing the main equations is not a problem until now, the big challenge comes when implementing the boundary equation of sensing molecules, namely:

$$\frac{\partial S}{\partial r}(1,t) - (L - M\int_0^1 B(r,t)dr) = 0, \tag{30}$$

where the equation needs to be defined at a specified value of $r$, while the integral $\int_0^1 B(r,t)dr$ needs to be calculated over all the interval of $r$-values, i.e. $[0,1]$. To solve this problem, we define an intermediate function $\pi(r,t)$ that does not appear in any of our equations except at the boundary condition of sensing molecules when $r = 1$. For that, we need to build the function $\pi$ such that:

$$\pi(1,t) = \int_0^1 B(r,t)dr. \tag{31}$$

This means that the intermediate function $\pi(1,t)$ and the value of $\int_0^1 B(r,t)dr$ are the same at the boundary. Since the integral value is the same as the value of $\pi$ at the points when $r = 1$, there is no need to express the integral in the boundary conditions. We will rather use the value of $\pi$ which resulted from solving the following system:

$$\begin{cases} D\dfrac{\partial \pi}{\partial t} = \dfrac{\partial^2 \pi}{\partial r^2} - \dfrac{\partial B}{\partial r}, \quad 0 < r < 1,\ t > 0, \\ \pi(0,t) = 0, \quad \dfrac{\partial \pi}{\partial r}(1,t) - B(1,t) = 0, \quad t > 0, \\ \pi(r,0) = rB_0, \quad 0 < r < 1. \end{cases} \tag{32}$$

We consider that $D = 0$ and we solve system (32) to get:

$$\pi(r,t) = \int_0^r B(x,t)dx, \tag{33}$$

which will be used in the numerical simulation instead of the complicated system (29) we had at first. Some of the numerical results are shown in Fig. 3 and Fig. 4.

Figure 3 shows that bacterial density distribution is changing its curve over time, the peak is decreasing and the shape is changing from uniform at the beginning, to a Gaussian shape then to a uniform almost equal to zero. The total density is decreasing over time and approaching zero. Figure 4 depicts the sensing molecules concentration profile starting at zero and then getting larger, especially near the boundaries. The biological interpretation of these results is that bacterial distribution profile changes as far as bacteria get stuck to the surface. The distribution becomes of a Gaussian shape when sensing molecules concentration is still relatively small. Once the amount of bacteria stuck is large, more sensing molecules are produced at the surface which leads to more attracted bacteria. This fact explains that the transition from Gaussian shape to a uniform again but this time with a decrease in the total bacterial density, which means that the majority of the population is at the surface and only a negligible amount remain in the free-space.

7. **Adding growth to the coupled model of chemotaxis.** In this section, we consider a growing population of bacteria. The model is presented in one dimensional space $[0,1]$ which is considered to be symmetric with respect to $x = 1/2$. The biological assumption added to the model is that bacteria is performing a logistic growth in the free-space and at the surface, for that the equations have the following form:

$$\begin{cases} \dfrac{\partial b}{\partial t} = D_b \dfrac{\partial^2 b}{\partial x^2} - \chi \dfrac{\partial}{\partial x}\left(b \dfrac{\partial s}{\partial x}\right) + abF(b), & 0 < x < 1,\ t > 0, \\ \dfrac{\partial s}{\partial t} = D_s \dfrac{\partial^2 s}{\partial x^2} - \lambda s + \alpha b, & 0 < x < 1,\ t > 0, \\ \dfrac{db_{wall}}{dt} = a b_{wall} F(b_{wall}) + \mu g(t), & t > 0, \\ b(0,t) = b(1,t) = 0, & t > 0, \\ D_s \dfrac{\partial s}{\partial x}(0,t) + \beta b_{wall}(t) = 0, & t > 0, \\ D_s \dfrac{\partial s}{\partial x}(1,t) - \beta b_{wall}(t) = 0, & t > 0, \\ b(x,0) = b_0,\ s(x,0) = s_0,\ b_{wall}(0) = b_{wall0}, & 0 < x < 1, \end{cases} \tag{34}$$

where $a$, $K$ and $\mu$ are the bacterial growth rate, bacterial carrying capacity, and fixed rate of bacterial stickiness respectively (see Table 1), while $g(t)$ is the proportion of bacteria stuck to the surface at each time $t$. For the logistic growth we define: $F(b) = 1 - b/K$. Since we are dealing with a growing population of bacteria, we remark that the expression of bacterial density at the surface is no more the total density minus the stuck-bacteria, we rather need to solve an ordinary differential equation to obtain bacterial density at the surface. Moreover, we derive $g(t)$ from the equation representing the total bacterial density in the free-space that says that the change in bacterial density at a given time results from the growth and death

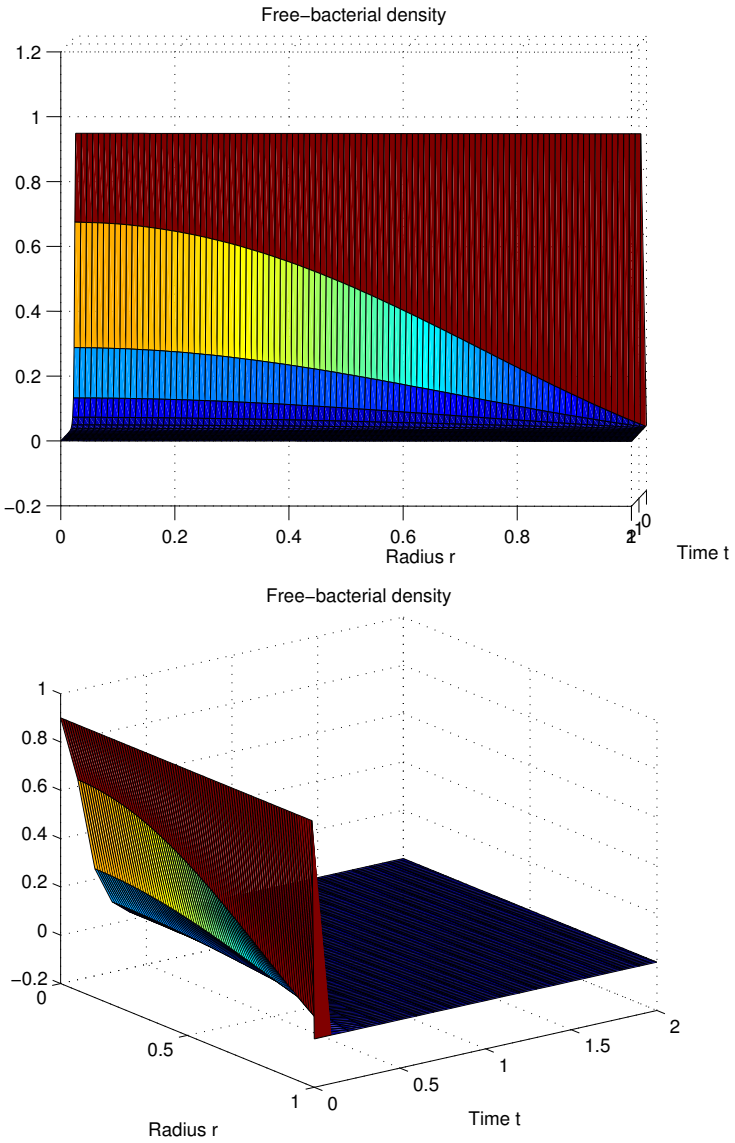


FIGURE 3. Two views of free-bacterial density distribution profile in space, as well as the density evolution in time, for $R = 1$, $\tau = 2.5$, $L = 0.75$ and $M = 0.7$. The top graph shows that bacterial distribution starts uniform and become of a Gaussian distribution shape to end up uniform that is almost zero everywhere. The bottom plot shows the free-bacterial density evolution over time which is the total density at the starting point and approaches zero as more bacteria stick to the surface with time.

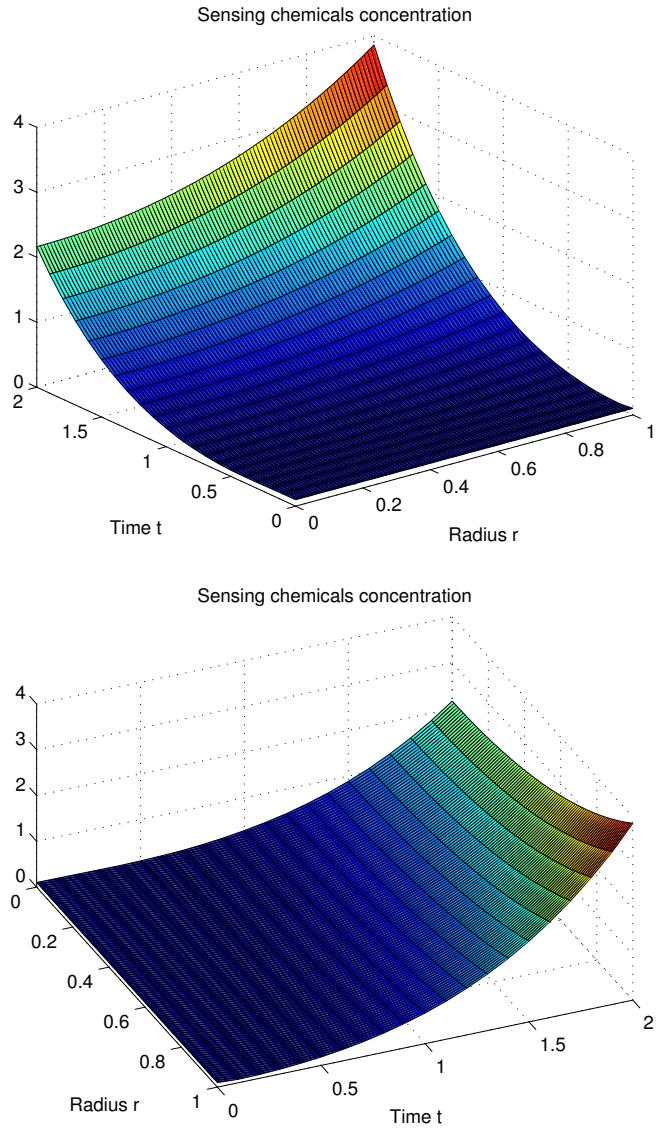


FIGURE 4. Sensing molecule distribution profile in space (top graph) and evolution in time (bottom graph), for $R = 1$, $\tau = 2.5$, $L = 0.75$ and $M = 0.7$. The top graph shows that the sensing molecules distribution starts very low then increases everywhere except that it is much higher near the surface. For the bottom graph, it shows that the sensing molecules concentration increases exponentially with time.

of bacteria within the free-space in addition to the bacteria lost and stuck to the surface, this is represented by the following:

$$\frac{\partial}{\partial t}\int_0^1 b dx = \underbrace{a\int_0^1 b(1-b/K)dx}_{Bacterial\ growth} - \underbrace{g(t)}_{Stuck-Bacteria},$$

$$\Rightarrow \int_0^1 \frac{\partial b}{\partial t}dx = a\int_0^1 b(1-b/K)dx - g(t),$$

$$\Rightarrow \int_0^1 \{D_b\frac{\partial^2 b}{\partial x^2} - \chi\frac{\partial}{\partial x}(b\frac{\partial s}{\partial x}) + ab(1-b/K)\}dx = a\int_0^1 b(1-b/K)dx - g(t),$$

$$\Rightarrow \left[D_b\frac{\partial b}{\partial x} - \chi(b\frac{\partial s}{\partial x})\right]_{x=0}^{x=1} + \int_0^1 ab(1-b/K)dx = a\int_0^1 b(1-b/K)dx - g(t),$$

$$\Rightarrow \left[D_b\frac{\partial b}{\partial x} - \chi(b\frac{\partial s}{\partial x})\right]_{x=0}^{x=1} = -g(t),$$

using the fact that $b(0,t) = b(1,t) = 0$, we obtain the following,

$$D_b\left[\frac{\partial b}{\partial x}(1,t) - \frac{\partial b}{\partial x}(0,t)\right] = -g(t),$$

since our variables are symmetric we have that $\frac{\partial b}{\partial x}(1,t) = -\frac{\partial b}{\partial x}(0,t)$, which lead to,

$$g(t) = 2D_b\frac{\partial b}{\partial x}(1,t). \tag{35}$$

As in section 5, we need to non-dimensionalize the model in order to determine the relative importance of the mechanisms involved. We denote non-dimensional quantities with hats and we rescale the variables using:

$$t = t^*/a,\ x = x^*/a,\ b = Kb^*,\ s = \frac{\alpha K}{a}s^*,\ b_{wall} = Kb^*_{wall},\ F(b) = F^*(b^*);$$

we note that $F^*(b^*) = 1 - b^*$, which means that after the non-dimensionalization the carrying capacity of bacteria becomes 1, and the system of equations become:

$$\begin{cases}
\frac{\partial b^*}{\partial t^*} = D_b^*\frac{\partial^2 b^*}{\partial x^{*2}} - \chi^*\frac{\partial}{\partial x^*}(b^*\frac{\partial s^*}{\partial x^*}) + b^*F^*(b^*), & 0 < x^* < 1,\ t^* > 0,\\
\frac{\partial s^*}{\partial t^*} = D_s^*\frac{\partial^2 s^*}{\partial x^{*2}} - \lambda^* s^* + b^*, & 0 < x^* < 1,\ t^* > 0,\\
\frac{db^*_{wall}}{dt^*} = b^*_{wall}F^*(b^*_{wall}) + \mu^*\frac{\partial b^*}{\partial x^*}(1,t^*), & t^* > 0,\\
b^*(0,t^*) = b^*(1,t^*) = 0, & t^* > 0,\\
\frac{\partial s^*}{\partial x^*}(0,t^*) + \beta^* b^*_{wall}(t^*) = 0, & t^* > 0,\\
\frac{\partial s^*}{\partial x^*}(1,t^*) - \beta^* b^*_{wall}(t^*) = 0, & t^* > 0,\\
b^*(x^*,0) = b_0^*,\ s^*(x^*,0) = s_0^*,\ b^*_{wall}(0) = b^*_{wall0}, & 0 < x^* < 1,
\end{cases} \tag{36}$$

where $D_s^* = aD_s$, $D_b^* = aD_b$, $\chi^* = \alpha K\chi$, $\lambda^* = \lambda/a$, $\mu^* = 2\mu D_b$ and $\beta^* = \beta/\alpha D_s$.

Furthermore, we drop the hats for simplicity and we implement the model. We use *FiPy* which is an object oriented, partial differential equation (PDE) solver, written in *Python*. *FiPy* uses the Finite Volume Method (FVM), a method for writing PDE's in the form of algebraic equations [53]. The name "Finite Volume"

refers to the small volume surrounding each node point on a mesh. The method uses Gauss' Divergence Theorem to convert volume integrals in a partial differential equation that contains a divergence term to a surface integrals. Then the terms are evaluated as fluxes at the surfaces of each finite volume. The method is easily formulated to allow for unstructured meshes and it is conservative, since the flux entering the volume is identical to the one leaving the adjacent volume.

In one-dimensional space, the finite volume method is based on subdividing the spatial domain into intervals (the " finite volume" also called *grid cells*) and finding an approximation to the integral of the functions over each of these volumes. In each time step we update these values using approximations to the flux through the endpoints of the intervals.

Using *Fipy* we simulate the mathematical model for $\lambda = 0.2$, $\mu = 0.3$, $\chi = 0.9$, $\beta = 0.5$, $D_s = 0.5$ and $D_b = 0.25$. In Fig. 5 shows the sensing molecules concentration profile, whereas in Fig. 6 depicts the bacterial density in the free-space and at the surface as well as sensing molecules concentration evolution in time.

Even with a growing population of bacteria, the density is almost zero as time gets larger so that the bacteria accumulates at the surface to start growing as a biofilm. This fact also explains the shape that takes sensing molecules concentration at the final time step, as we can see in Fig. 5 the concentration is much higher near the surface because of the high production near the surface and the low production in the free-space. Fig. 6 shows that free-bacterial density takes a long time before dropping to zero. This means that bacterial growth has kept bacteria in the free-space longer. While stuck-bacteria also grow so that their density increases, their growth is still bellow the carrying capacity. Being produced by both free and stuck-bacteria, sensing molecules concentration is exponentially increasing. This would attract more bacteria to the surface and facilitate biofilm initiation.

## 8. **Conclusion.**

In this work, we considered a high bacterial population, so that the amount of sensing molecules produced by the bacteria to sense their proximity to the surfaces is significant. We presented a coupled mathematical model of Keller-Segel type, representing bacterial density and sensing molecules concentration, in one-dimensional space. Bacteria perform a random movement directed by the sensing molecules attractant. The sensing molecules diffuse, degrade and are produced by both bacterial populations, at the surface and in the free-space. We started by a fixed population of bacteria, then we added bacterial growth to our model later on. It was very challenging to define the boundary equations for sensing molecules, since they get produced at the surface, they degrade and then diffuse and none of these behaviors could be neglected in the equation describing the boundary conditions. The model's equations are very complicated to be studied analytically, so one way of studying this model is through numerical analysis.

Our results show that bacterial density starts as a uniform distribution within a well defined medium, then search for surfaces to stick to it. Since we placed the surface at the boundaries, we remarked that as bacteria get stuck, the shape of bacterial density distribution changes to a Gaussian before to return back to a uniform, this time almost zero everywhere. This means that the majority of bacteria are stuck to the surface, the fact that agrees with the biological description the nature of bacterial life given in [30]. Studies in [30] show that the free-living bacteria look for, whether a living or non-living surface to stick before aggregating

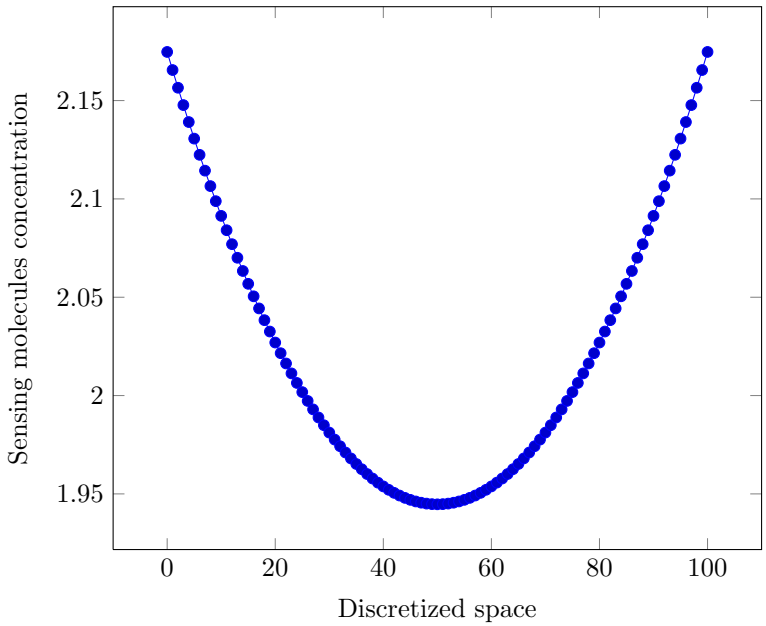


FIGURE 5. sensing molecules distribution profile in a discretized interval $[0, 1]$, at the final time step $T = 40000$. The simulation started with a very low amount of sensing molecules present in the free-space $s_0 = 0.01$ uniformly distributed.

as a biofilm. They also explained the result showing the evolution of the total bacterial density in time that approaches to zero as time gets larger, which means the density distribution is almost zero everywhere.

Bacteria use sensing molecules to sense their proximity to the surface before they attach to it [30]. This fact was also included in our model as chemotaxis, which means that bacterial movement is a random walk directed by the sensing molecules attractant. For sensing molecules, our results show that their concentration gets higher near the surface as time goes on. Since the sensing molecules are produced by bacteria and that bacterial density gets larger at the surface then the production at the surface is much higher than the production in the free-space. The presence of highly concentrated sensing molecules near the surface is essential for biofilm construction. The bacteria will move towards the high concentration of sensing molecules, get stuck to the surface and then keep producing the sensing molecules to attract other bacteria to join the aggregation. This is explained by the increasing sensing molecules concentration with time obtained by showing sensing molecules concentration evolution in time.

Our work gives rise to results that agree with the biological description of the early stages of biofilm formation. However, our model does not include some important elements that participate in building biofilm such as bacterial nutrients and temperature. Of course, including such elements will make the model more realistic but also more complex to study and analyze. Still, a more relevant work would be to do real experiments for one or more bacterial species and look at their biofilm

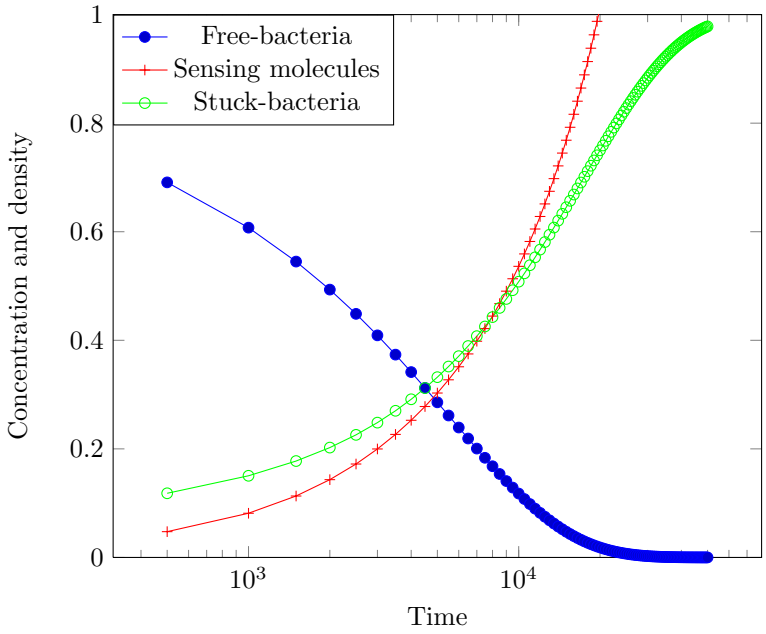


FIGURE 6. the evolution of bacterial density in the free-space and at the surface with the sensing molecules concentration. We start with bacteria in the free-space that stick to the surface so that the density in the free-space drop to zero and the density at the surface increases until it reaches the carrying capacity, for sensing molecules they are produced by both free and stuck bacteria thus they increase exponentially.

initiation then compare the experimental results to the mathematical model, after that we will be able to manipulate bacterial behavior through mathematical studies.

For our model to be more useful in a medical or industrial point of view, we hope to extend it to study the inhibition of the bacterial attachment to surfaces. This model will help us to manipulate biofilm formation depending on our needs, either to accelerate it formation when it is beneficial or to inhibit its growth when it is bad. Other perspectives of our work could be to model the next step that is the reversible attachment which consists of bacterial swarming.

The aim of our work was to model biofilm initiation and bacterial movement toward surfaces. We developed an appropriate boundary conditions that describe this phenomenon.

**Acknowledgments.** Fadoua El Moustaid would like to express her sincere gratitude to the African Institute for Mathematical Sciences (AIMS) in South Africa for the scholarship that funded her Masters degree and for what she learned throughout her post-graduate studies which has greatly impacted her graduate research experience. Amina Eladdadi would like to acknowledge the funding from NSF to participate in the US-South Africa workshop on mathematical methods in systems biology and population dynamics organized by Urszula Ledzewicz, which resulted in this collaboration.

## REFERENCES


[1] A. Bejan, "Convection Heat Transfer," John Wiley and Sons Inc., New York, NY Publisher, 1984.

[2] A. Coghlan, *Slime city*, New Scientist, **151** (1996), 32–36.

[3] A. P. Petroff, TD. Wu, B. Liang, J. Mui, JL. Guerquin-Kern, H. Vali, D. H. Rothman and T. Bosak, *Reaction diffusion model of nutrient uptake in a biofilm: Theory and experiment*, Journal of Theoretical Biology, **289** (2001), 90–95.

[4] C. D. Nadell, J. B. Xavier and K. R. Foster, *The sociobiologyof biofilms*, FEMS Microbiol Review, (2009) 1–19.

[5] C. Picioreanu, M. C. M. Van Loosdrecht and J. J. Heijnen, *Mathematical modeling of biofilm structure with a hybrid differential-discrete cellular automaton approach*, Biotechnology and Bioengineering, **58** (1997).

[6] C. S. Laspidou, A. Kungolos, P. Samaras C. S. Laspidou, A. Kungolos and P. Samaras, *Cellular-automata and individual-based approaches for the modeling of biofilm structures: Pros and cons*, Journal of Desalination, **250** (2010), 390–394.

[7] D. Horstmann, *From 1970 until present: The Keller-Segel model in chemotaxis and its consequences*, 2003.

[8] D. Jones, V. K. Hristo and D. Le and H. Smith, *Bacterial wall attachment in a flow reactor*, SIAM Journal, **62** (2002), 1728–1771.

[9] D. Priscilla, *Biofilms: The environmental playground of Legionella pneumophila*, Journal of Environmental Microbiology, **12** (2010), 557–566.

[10] D. V. Nicolau Jr., J. P. Armitage and P. K. Maini, *Directional persistence and the optimality of run-and-tumble chemotaxis*, Computational Biology and Chemistry, **33** (2009), 269–274.

[11] E. A. J. F. Peters and Th. M. A. O. M. Barenbrug, *Efficient brownian dynamics simulation of particles near walls. I. Reflecting and adsorbing walls*, Physical Review E, **66** (2002).

[12] E. A. J. F. Peters and Th. M. A. O. M. Barenbrug, *Efficient brownian dynamics simulation of particles near walls. II. sticky walls*, Physical Review E, **66** (2002).

[13] E. Ben Jacob, O. Schochet, A. Tenenbaum, I. Cohen, A. Czirok and T. Vicsek, *Generic modelling of cooperative growth patterns in bacterial colonies*, Nature Journal, **368** (1994), 46–49.

[14] E. F. Keller, *Science as a medium for friendship: How the Keller-Segel models came about*, Bull. Math. Biol., **68** (2009), 1033–1037.

[15] E. F. Keller and L. A. Segel, *Initiation of slide mold aggregation viewed as an instability*, Journal of Theoretical Biology, **26** (1970), 399–415.

[16] E. F. Keller and L. A. Segel, *Model for chemotaxis*, Journal of Theoretical Biology, **30** (1971), 225–234.

[17] E. F. Keller and L. A. Segel, *Traveling bands of chemotactic bacteria: A theoretical analysis*, Journal of Theoretical Biology, **30** (1971), 235–248.

[18] G. D. Zacarias, C. P. Ferreira and J. X. Velasco-Hernandez, *Porosity and tortuosity relations as revealed by a mathematical model of biofilm structure*, Journal of Theoretical Biology, **233** (2005), 245–251.

[19] H. Donnelly, *Uniqueness of positive solutions of the heat equation*, American Mathematical Society, **99** (1987).

[20] H. F. Jenkinson and H. M. Lappin-Scott, *Biofilms adhere to stay*, Journal of Trends in Microbiology, **9** (2001), 9–10.

[21] H. Stoodley, Luanne, W. Costerton and P. Stoodley, *Bacterial biofilms: From the natural environment to infectious diseases*, Review of Microbiology, **2** (2004), 1740–1526.

[22] H. Tamboto, K. Vickery and A. K. Deva, *Subclinical (Biofilm) infection causes capsular contracture in a porcine model following augmentation mammaplasty*, Plastic & Reconstructive Surgery, **126** (2010), 835–842.

[23] I. Klapper and J. Dockery, *Mathematical description of microbial biofilms*, SIAM Journal, **52** (2010), 221–265.

[24] J. D. Murray, "Mathematical Biology II: Spatial Models and Biomedical Applications," S. S. Antman editor, Springer Publisher, 2003.

[25] J. D. Murray, "Mathematical Biology I: An Introduction," S. S. Antman editor, Springer publisher, 2002.

[26] J. E. Guyer, D. Wheeler and J. A. Warren, *FiPy: Partial differential equations with python*, Journal of Computer Science and Engineering, **11** (2009), 6–15.

[27] J. L. Goldberg and A. J. Schwartz, "Systems of Ordinary Differential Equations: An Introduction," I. N. Herstein and Gian-Carlo Rota editor Harper and Row publisher.
[28] J. S. Poindexter and E. R. Leadbetter, " Bacteria in Nature 2: Methods and Special Applications in Bacterial Ecology," Spring Street Editor, Plenum Press, New York, 1986.
[29] J. W. Costerton, *Overview of microbial biofilms*, Journal of Industrial Microbiology and Biotechnology, **15** (1995), 137–140.
[30] J. W. Costerton, *Introduction to biofilm*, International Journal of Antimicrobial Agents, **11** (1999), 217–221.
[31] J. W. Costerton, G. G. Geesey and G. K. Cheng, *How bacteria stick*, Sci. Am., **238** (1978), 86–95.
[32] KJ. Engel, R. Nagel. "One Parameter Semigroups for Linear Evolution Equation," S. Axler editor, Springer publisher, 2000.
[33] K. K. Jefferson, *What drives bacteria to produce a biofilm?*, FEMS Microbiology Letters, **236** (2004), 163–173.
[34] K. Kang, T. Kolokolnikov and J. Ward, *The stability and dynamics of a spike in the 1D Keller Segel model*, IMA Journal of Applied Mathematics, (2007).
[35] K. Kawasaki, A. Mochizuki, M. Matsushita, T. Umeda and N. Shigesada, *Modeling spatio-temporal patterns generated by bacillus subtilis*, Journal of Theoretical Biology, **188** (1997), 177–185.
[36] K. Sauer, A. K. Camper, G. D. Ehrlich, J. W. Costerton and D. G. Davies, *Pseudomonas aeruginosa displays multiple phenotypes during development as a biofilm*, Journal of Bacteriology, **184** (2002), 1140–1154.
[37] L. R. Johnson, *Microcolony and biofilm formation as a survival strategy for bacteria*, Journal of Theoretical Biology, **251** (2008), 24–34.
[38] M. Ballyk and H. Smith, *A model of microbial growth in a plug flow reactor with wall attachment*, Mathematical Biosciences, **158** (1999), 95–126.
[39] M. Burmolle, T. Rolighed Thomsen, M. Fazli, I. Dige, L. Christensen, P. Homoe, M. Tvede, B. Nyvad, T. Tolker-Nielsen, M. Givskov, C. Moser, K. Kirketerp-Moller, H. Krogh Johansen, N. Hoiby, P. Ostrup Jensen, S. J. Sorensen and T. Bjarnsholt, *Biofilms in chronic infections a matter of opportunity monospecies biofilms in multispecies infections*, FEMS Immunol. Med. Microbiol, **59** (2010), 324–336.
[40] M. G. Fagerlind, J. S. Webb, N. Barraud, D. McDougald, A. Jansson, P. Nilsson, M. Harln, S. Kjelleberg and S. A. Rice, *Dynamic modelling of cell death during biofilm development*, Journal of Theoretical Biology, **259** (2012), 23–36.
[41] M. M. Ballyk, D. A. Jones and H. L. Smith, *Microbial competition in reactors with wall attachment*, Microbial Ecology, **41** (2001), 210–221.
[42] M. Mimura, H. Sakaguchi and M. Matsushita, *Reaction diffusion modeling of bacterial colony patterns*, Physica A: Statistical Mechanics and its Applications, **282** (2000), 283–303.
[43] M. R. Rahbar, I. Rasooli, S. Latif, M. Gargari, J. Amani and Y. Fattahian, *In silico analysis of antibody triggering biofilm associated protein in Acinetobacter baumannii*, Journal of Theoretical Biology, **266** (2010), 275–290.
[44] M. Tindall, P. Maini, S. Porter and J. Armitage, *Overview of mathematical approaches used to model bacterial chemotaxis II: Bacterial populations*, Bulletin of Mathematical Biology, **70** (2008), 1570–1607.
[45] N. Balaban, "Control of Biofilom Infections by Signal Manipulation," J. William Costerton Editor Springer Publisher, 2008.
[46] N. Hoiby, T. Bjarnsholt, M. Givskov, S. Molin and O. Ciofu, *Antibiotic resistance of bacterial biofilms*, International Journal of Antimicrobial Agents, **35** (2010), 322–332.
[47] N. Hoiby, T. Bjarnsholt, M. L. Givskov, S. Molin and O. Ciofu, *Antibiotic resistance of bacterial biofilms*, International Journal of Antimicrobial Agents, **35** (2010), 322–332.
[48] O. Wanner and W. Gujer, *A multispecies biofilm model*, Biotechnology and Bioengineering, **28** (1986), 314–328.
[49] P. Carol, *Microbiology: Biofilms invade microbiology*, Journal of Science, **273** (1996), 1795–1797.
[50] P. Watnick and R. Kolter, *Biofilm, city of microbes*, Journal of Bacteriology, **182** (2000), 2675–2679.
[51] Q. Wang and T. Zhang, *Review of mathematical models for biofilms*, Solid State Communications, **150** (2010), 21–22.

[52] R. Erban and G. Othmer, *From signal transduction to spatial pattern formation in E. coli: A paradigm for multiscale modeling in biology, multiscale model*, Journal of Simul., **3** (2005), 362–394.
[53] R. J. Leveque, "Finite Volume Methods for Hyperbolic Problems," Cambridge University Press, 2002.
[54] R. M. Donlan and J. W. Costerton, *Survival mechanisms of clinically relevant microorganisms*, Clinical Microbiology Reviews, **15** (2002).
[55] T. R. de Kievit, *Quorum sensing in Pseudomonas aeruginosa biofilms*, Environmental Microbiology, **11** (2009), 279–288.
[56] T. Tolker-Nielsen, U. C. Brinch, P. C. Ragas, J. B. Andersen, C. S. Jacobsen and S. Molin, *Development and dynamics of Pseudomonas sp. biofilms*, Journal of Bacteriology, **182** (2000).
[57] S. Abdul Rani, B. Pitts, H. Beyenal, R. A. Veluchamy, Z. Lewandowski, W. M. Davison, K. Buckingham-Meyer and P. S. Stewart, *Spatial patterns of DNA replication, protein synthesis, and oxygen concentration within bacterial biofilms reveal diverse physiological states*, Journal of Bacteriology, **189** (2007), 4223–4233.
[58] Z. Lewandowski and H. Beyenal, *Mechanisms of microbially influenced corrosion*, Springer Berlin Heidelberg, **4** (2009), 35–64.
[59] http://grants.nih.gov/grants/guide/pa-files/PA-03-047.html Last Accessed on June 11, 2012.

Received June 03, 2012; Accepted January 07, 2013.

*E-mail address*: elmousfa@mail.uc.edu
*E-mail address*: eladdada@strose.edu
*E-mail address*: lafras@aims.ac.za